

The Phase Diagram of Disordered Vortices from London Langevin Simulations

Anne van Otterlo[†], Richard T. Scalettar and Gergely T. Zimányi
Physics Department, University of California, Davis, CA 95616, USA
 (February 18, 1998)

We study the phase diagram of vortex matter in disordered type-II superconductors. We performed numerical simulations in the London Langevin approximation, using a new realistic representation of the disorder. At low magnetic fields we find a disentangled and dislocation free Bragg-glass regime. Increasing the field introduces disorder-driven entanglement in a discontinuous manner, leading to a vortex-glass phase, which subsequently melts into the vortex liquid. The obtained phase boundaries are in quantitative agreement with the experimental data.

PACS numbers: 74.60.Ge, 74.25.Dw

Fluctuations in the High Temperature Superconductors (HTSC) play a dominant role in vortex phenomenology due to the high transition temperatures $T_C \sim 100\text{K}$ and large anisotropies $\epsilon^{-1} \sim 5\text{-}500$. As a result, in clean systems the Abrikosov lattice melts into an entangled vortex liquid with increasing temperature. This transition was predicted on the basis of Lindemann type calculations [1,2] and is by now firmly established by London [3], 3D XY [4], and Ginzburg-Landau [5] simulations. Experimentally, the latent heat found in YBCO [6] and the jump in the magnetization in BSSCO [7,8] and YBCO [9,10] provide thermodynamic evidence for a first order melting transition at low fields.

Although disorder was first argued to eliminate the long range order of the Abrikosov lattice altogether [11], more recent theories propose that quasi-long-range translational order is still preserved at low magnetic fields in a dislocation free ‘‘Bragg-glass’’ phase [12,13]. Increasing the field effectively increases the disorder and as the pinning energies overcome the elastic energies, vortices entangle [14] forming a vortex-glass [15]. Experimental support for this scenario is the sharp enhancement of the critical current from magnetization measurements [16–19], the rapid destruction of the Bragg peaks in neutron scattering [20], and the pronounced dips in the I-V curves [21]. A numerical study found evidence for pairs of point-like disclination defects driving the Bragg-glass to vortex glass transition in layered systems with strong pins [22]. Transport measurements [23,24] indicate that the first order melting transition from the Bragg-glass to the vortex liquid at low fields is replaced by a continuous melting transition from the vortex glass to the vortex liquid at higher fields. This basic feature is reproduced by numerical simulations [25,26]. Whether the vortex glass and vortex liquid are separated by a phase transition or a crossover is presently under discussion and seems to depend on the screening length [27].

In this Letter we report continuum Langevin simulations for disordered vortex systems in the London approximation, which is valid outside the 3D XY critical region and for fields $B \lesssim 0.2H_{c2}(T)$. This approach is more realistic than lattice simulations due to the absence

of intrinsic pinning, yet it is capable of reaching satisfactory system sizes. Furthermore, by using a coarse grained pinning landscape, we are able to reach the weak collective pinning regime. We measure the in-plane structure factor $S(\mathbf{Q})$, the vortex wandering along the field $B(z)$, as well as the time overlap correlator $C(t)$ (see below for the definitions of these quantities). The central result of our paper is the determination of the phase diagram for realistic YBCO parameters (Fig. 1).

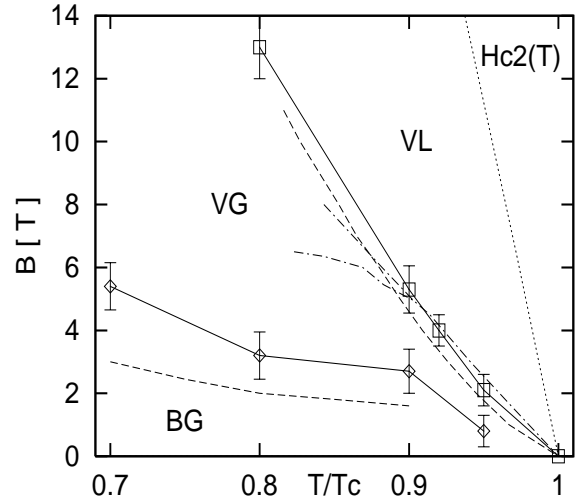


FIG. 1. The B - T phase diagram for YBCO parameters, consisting of a Bragg Glass, Vortex Glass, and Vortex Liquid phases. For comparison, experimental data is shown as dashed (Ref. [19]) and dash-dotted (Ref. [21]) lines.

We start by outlining our numerical approach. The magnetic field is taken to be in the c -direction, perpendicular to the CuO_2 -layers, indexed by z . The Langevin equation describing the overdamped motion of vortices reads

$$\eta \frac{\partial \mathbf{R}_\mu(z, t)}{\partial t} = \zeta_\mu(z, t) + \mathbf{F}_L - \frac{\delta H[\{\mathbf{R}_\nu(z, t)\}]}{\delta \mathbf{R}_\mu(z, t)}, \quad (1)$$

where μ labels the vortices with coordinates \mathbf{R} . The damping force on the left hand side is characterized by the coefficient η that is related to the Bardeen-Stephen flux-flow resistivity by $\rho_{\text{BS}} = B\Phi_0/(c^2\eta)$, where $\Phi_0 = hc/2e$

is the flux quantum. The Langevin force ζ is correlated as $\langle \zeta_\mu^\alpha(z, t) \zeta_\nu^\beta(z', t') \rangle = 2\eta T \delta^{\alpha\beta} \delta_{\mu\nu} \delta(z - z') \delta(t - t')$, with $\alpha, \beta = x, y$. The Lorentz force from a bias current density \mathbf{J} is $\mathbf{F}_L = \Phi_0 \mathbf{J} \times \hat{\mathbf{z}}/c$. The Hamiltonian H is constructed on the basis of London theory. Its derivative decomposes into three forces. The pairwise interaction force is the periodic extension of the in-plane London interaction, in Fourier space $V(k) = 2\pi\epsilon_0 \exp(-k^2\xi^2)/(\lambda^{-2} + k^2)$, with line energy $\epsilon_0 = \Phi_0^2/(8\pi\lambda)^2$, London penetration depth λ , and coherence length ξ . We choose $\kappa = \lambda/\xi = 100$. The bending forces are governed by the single vortex elastic constant $c_{44} = \epsilon^2\epsilon_0 \log(\kappa)$, with anisotropy $\epsilon = 1/5$. Finally, the dimensionless pinning force on vortex μ in layer z for δT_C disorder is given by

$$\mathbf{F}_{\mu,z}^P = - \int d^2R' \nabla_{\mathbf{R}_\mu(z)} p(\mathbf{R}_\mu(z) - \mathbf{R}') u(\mathbf{R}', z), \quad (2)$$

where the microscopic disorder potential is delta-correlated, $\langle u(\mathbf{R}, z) u(\mathbf{R}', z') \rangle = \gamma \delta(\mathbf{R} - \mathbf{R}') \delta_{z,z'}$, with strength γ . With our conventions, the parameter γ equals the parameter δ_α in Chapter III C of Ref. [2]. The convolution with the long-range vortex form factor $p(R) = 2\xi^2/(R^2 + 2\xi^2)$ generates a smooth pinning landscape.

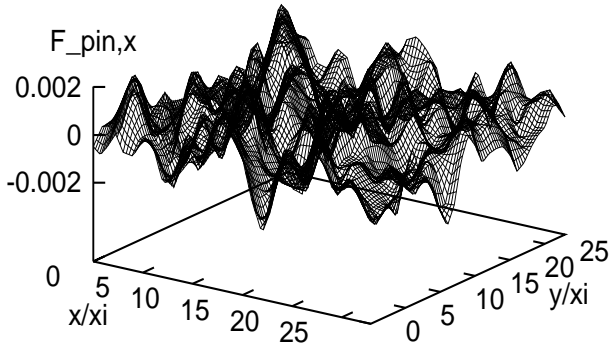


FIG. 2. A part of a typical pinning landscape (“pinscape”). Shown is the pinning force in the x -direction.

The z coordinate is discretized with the natural layer spacing $d \approx 12\text{\AA}$. The total number of layers in the z -direction is denoted by L_z . We employ *open* boundary conditions in this direction, which allows topological defects to enter the sample from the top and bottom. The in-plane coordinates \mathbf{R}_μ satisfy periodic boundary conditions and lie in a parallelogram spanned by the unit vectors $\hat{e}_a = \hat{e}_x$ and $\hat{e}_b = (\hat{e}_x + \sqrt{3}\hat{e}_y)/2$ with area given by the number of vortices N times Φ_0/B . The unit of length is taken to be the coherence length $\xi(T)$, with $\xi(0) = 17\text{\AA}$, so that $H_{c2}(0) = 120\text{T}$; the average inter-vortex distance is a_Φ . The natural unit of time is $t_0 = \xi^2\eta/\epsilon_0$ and the time t is discretized with timestep δt_0 ; we take $\delta = 0.05$. We mention two technical aspects of importance. Considerable gain is reached in computational speed by generating and storing the pinning forces (the “pinscape”, see Fig. 2) on a regular array of spacing ξ . The pinning

force at a specific vortex location is then constructed by interpolating between the four closest grid-points. Second, in order to equilibrate disordered systems, we employed simulated annealing, cooling from $\sim 2.5T$ to T in 10 % decrements. Most of our simulations were done for 7×7 vortices in 50 layers, using 100,000 sweeps for equilibration and 100,000 for measurement. With the exceptions below we found only limited fluctuations between different disorder configurations, due to the good self-averaging of the ~ 2500 vortex elements. Therefore, typically we averaged over only a few disorder realizations. Finally the disorder strength was chosen to yield reasonable low temperature values for the critical current in terms of the depairing current j_0 : $j_c/j_0 \sim 0.005$.

We now proceed to investigate the transitions between the three proposed phases, the dislocation free Bragg Glass (BG), the dislocated Vortex Glass (VG), and the Vortex Liquid (VL).

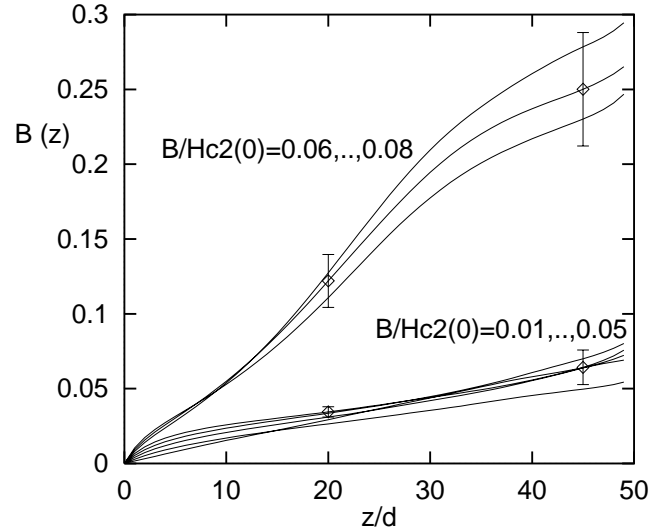


FIG. 3. The vortex wandering $B(z)$ in the z -direction for different magnetic fields at $T/T_c = 0.7$, $\gamma = 0.1$, and $\epsilon = 0.2$ shows the Bragg to Vortex Glass transition.

The BG-VG transition. In the dislocation-free Bragg Glass vortices fluctuate in the self-consistent cage of their neighbours [14]. Increasing the field brings vortices closer together, and increases the relative strength of the disorder. When the single vortex wandering reaches the Lindemann limit, vortices entangle and dislocations enter the sample [14,28]. Our measured vortex line wandering, $B(z) = \langle [\mathbf{R}_\mu(z, t) - \mathbf{R}_\mu(0, t)]^2 \rangle / a_\Phi^2$, is displayed in Fig. 3 for a typical field sweep. The curves for the five lowest fields group together and belong to the Bragg glass, whereas the curves for the higher fields are in the vortex glass phase. Our low field data in the BG in Fig. 3 grow slowly with z , and are consistent with a power law with exponent less than unity. The presently attainable system sizes are, however, too small to see the asymptotic regime, where $B(z) \sim \ln(z)$ [13]. Increasing the field across the transition enhances $B(z)$ abruptly and

instead of bending down, the curves now bend upward until boundary effects become important around $z \sim L_z$.

The vortex wandering in the VG phase reaches the Lindemann number c_L at the entanglement length in the z -direction L_E . From $B(L_E) \equiv c_L^2 \lesssim 0.1$, we deduce that just above the transition, the entanglement length is of the order of 15 lattice spacings in the z -direction for the parameters of Fig. 3. Thus, our system size in the z -direction (50) is large enough to see entanglement, as evidenced by the snapshot just inside the VG phase in Fig. 4b, which shows two entangled “ring-exchanges”, or screw-dislocation loops, involving 2 and 9 vortices. On the other hand, Fig. 4a, taken on the BG side of the transition shows a perfect disentangled lattice.

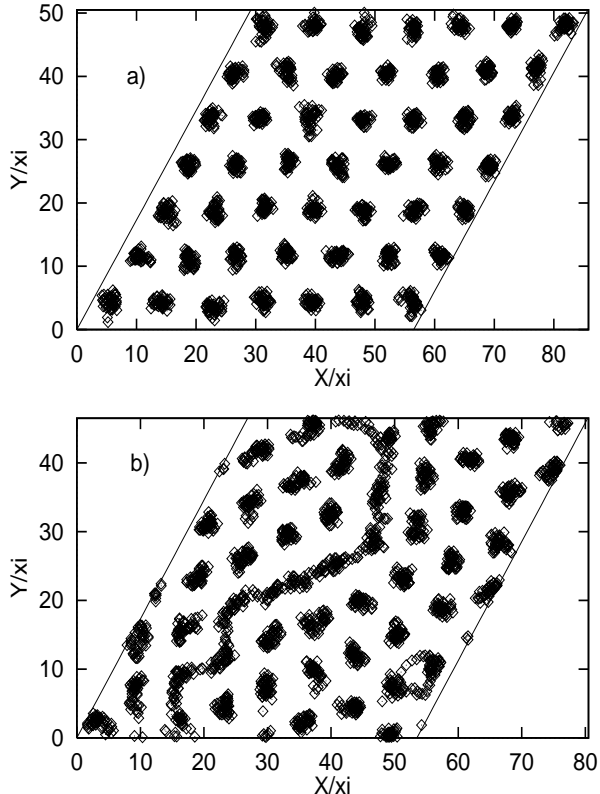


FIG. 4. Snapshots of a typical configuration projected in the xy -plane in the a) the Bragg glass phase at $B=6T$ and b) the Vortex Glass phase at $B=7.2T$. Parameters as for Fig. 3.

The average height of the six principle structure factor peaks in $S(\mathbf{Q}) = \langle (1/N) \sum_{\mu,\nu} \exp(i\mathbf{Q} \cdot [\mathbf{R}_\mu(z,t) - \mathbf{R}_\nu(z,t)]) \rangle$ is also indicative of the BG-VG transition. This is shown in Fig. 5, together with the wandering across the sample $B(L_z)$. In the BG phase, the structure factor first increases with field, due to the growing interaction strength. Upon crossing the BG-VG transition, the structure factor peak height drops at the same point where the wandering increases dramatically. Frozen-in short range order still persists in the VG phase, however, as is clear from Fig. 4b.

For different disorder realizations, the jump in $B(L_z)$

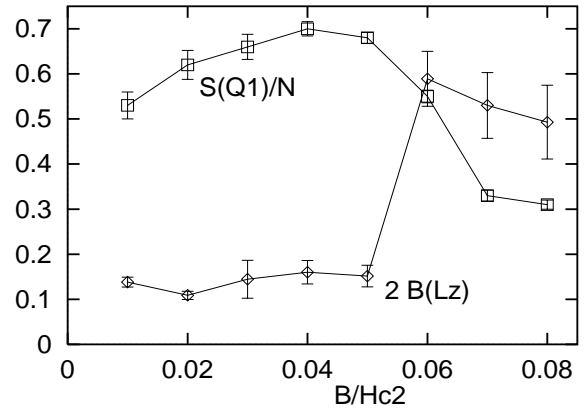


FIG. 5. The magnetic field dependence at $T/T_C=0.7$ of the averaged amplitude of the first 6 primary structure factor peaks (boxes), normalized to the number of vortices $N=49$, and the wandering across the sample $B(L_z)$ (diamonds).

and the corresponding drop of the structure factor peaks, occur at different magnetic fields. As a result, a disorder average of the quantities we measure shows only a smooth field dependence. Although the sharp jump in the wandering for a single disorder realization is consistent with a first order transition, we speculate that in the thermodynamic limit only a broad feature survives, which mimics a continuous transition or a cross-over.

VG-VL transition. This transition is defined by a profound change in the dynamical behavior of the system: the vortex glass can be seen as a frozen liquid. This is most clearly seen in the behavior of the time overlap correlator $C(t) = \exp(-\langle [\mathbf{R}_\mu(z,t) - \mathbf{R}_\mu(z,0)]^2 \rangle / l^2)$, as plotted for $l=0.2a_\Phi$ in the inset of Fig. 6. For times $t \gg t_0$ it decays exponentially with a “plastic” relaxation time t_{pl} , which is plotted as a function of temperature in Fig. 6. Upon cooling from the VL to the VG, the time t_{pl} rapidly increases, signalling that vortices get trapped in the almost static cages of the surrounding vortices. The plastic time does not appear to be infinite in the VG, however. It saturates for temperatures below the VG-VL line, at a value around $t_{pl} \sim 2000t_0$. Whether this is a finite size effect, or hints to the absence of a genuine phase transition with universal exponents, will be the subject of a future finite size study [29].

As a function of temperature and field, the six primary structure factor peaks decrease, but in the vortex-glass phase with frozen short range order, they remain finite and visible in our finite system and simulation time. As the vortex glass melts into the liquid, the primary peaks dissolve into a ringlike structure. Transport measurements can also identify the VG-VL transition. Fisher et al. [15] suggested that the flux flow resistivity at high temperature gives way to non-ohmic exponential creep below the glass transition temperature, a prediction which was confirmed experimentally [30], see, however,

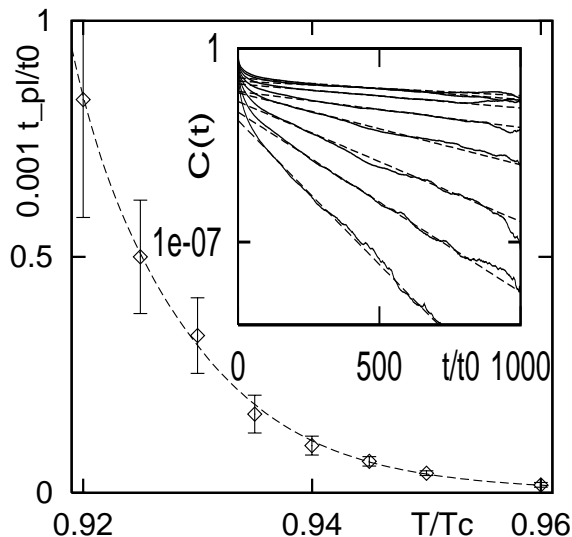


FIG. 6. The relaxation time $t_{pl}/(10^3 t_0)$ as a function of temperature from an exponential fit to the correlator $C(t)$ illustrates the VG-VL transition. Here $B=4T$ and the dashed line is a guide to the eye. The inset shows the correlation function $C(t)$ as a function of time for $T/T_c=0.91, \dots, 0.95$ (step 0.005, full lines, from top to bottom) and the fits (dashed lines).

also Ref. [31]. Our numerical results on the IV curves will be presented elsewhere [29].

The above diagnostics allow us to construct the phase diagram. We identified the predicted dislocation free Bragg Glass, entangled Vortex Glass, and Vortex Liquid phases in the B - T plane, as summarized in Fig. 1. We find that the BG-VG phase boundary is rather sensitive to the disorder, whereas the VG-VL transition is not. In fact, even from disorder realization to realization, the location of the BG-VG boundary shows detectable fluctuations. This sensitivity is a well known experimental fact: Safar et al. [21] report transition fields from $3T$ to $10T$ in samples with minute macroscopic differences, whereas the data of Ref. [17] are at even lower fields. Experimentally, the BG-VG transition appears as a sharp jump in the magnetization only in BSSCO, while in YBCO and Thallium based materials the transition is rather smooth. The reported numerical fluctuations seem to be related to this smearing of the BG-VG transition in the latter compounds. In Fig. 1 we also display the experimental data of Deligiannis et al. [19] and Safar et al. [21]. We chose a disorder value to make the transition field fall between the two sets of data. The correspondence between the simulations and experimental data is remarkable, especially for the VG-VL transition. At the highest temperatures $T/T_c \sim 0.95$, the BG-VG phase boundary bends downward. The resolution of our data is insufficient at the moment to decide, whether the BG-VG line ends somewhere on the melting line, as the BSSCO [8] and some YBCO data [21] indicates, or whether there is

a sliver of the VG phase intruding all the way down to zero fields, preempting a direct BG-VL transition, as the Thallium [16] and other YBCO data [17,19] suggests.

We thank G. Blatter, T. Giamarchi, P. Kes, and V. Vinokur for discussion. We gratefully acknowledge the hospitality of the ETH in Zürich (AvO) and of the Argonne National Laboratories (GTZ). This research was supported by NSF grant DMR 95-28535 and by the Dutch Foundation for Fundamental Research on Matter (FOM).

† Present address: Instituut-Lorentz for Theoretical Physics, P.O.B. 9506, 2300 RA Leiden, The Netherlands.

- [1] D. R. Nelson, Phys. Rev. Lett. **60**, 1973 (1988).
- [2] G. Blatter et al., Rev. Mod. Phys. **66**, 1125 (1994).
- [3] H. Nordborg and G. Blatter, Phys. Rev. Lett. **79**, 1925 (1997).
- [4] X. Hu, S. Miyashita, and M. Tachiki, Phys. Rev. Lett. **79**, 3498 (1997); S. Ryu and D. Stroud, Phys. Rev. Lett. **78**, 4629 (1997).
- [5] R. Sasik and D. Stroud, Phys. Rev. Lett. **75**, 2582 (1995); J. Hu and A. MacDonald, Phys. Rev. B **56**, 2788 (1997).
- [6] A. Schilling et al., Nature **382**, 791 (1996).
- [7] H. Pastoriza et al., Phys. Rev. Lett. **72**, 2951 (1994).
- [8] E. Zeldov et al., Nature **375**, 373 (1995).
- [9] R. Liang, D. A. Bonn, and W. N. Hardy, Phys. Rev. Lett. **76**, 835 (1996).
- [10] U. Welp et al., Phys. Rev. Lett. **76**, 4809 (1996).
- [11] A. I. Larkin and Yu. N. Ovchinnikov, Zh. Eksp. Teor. Fiz. **65**, 1704 (1973) [Sov. Phys. JETP **38**, 854 (1974)].
- [12] T. Natterman, Phys. Rev. Lett. **64**, 2454 (1990).
- [13] T. Giamarchi and P. Le Doussal, Phys. Rev. Lett. **72**, 1530 (1994); Phys. Rev. B **52**, 1242 (1995).
- [14] D. Ertas and D. R. Nelson, Physica C **272**, 79 (1996).
- [15] M. P. A. Fisher, Phys. Rev. Lett. **62**, 1415 (1989); D. S. Fisher, M. P. A. Fisher, and D. A. Huse, Phys. Rev. B **43**, 130 (1991).
- [16] V. Hardy et al., Physica C **232**, 347 (1994).
- [17] L. Klein et al., Phys. Rev. B **49**, 4403 (1994).
- [18] B. Khaykovich et al., Phys. Rev. Lett. **76**, 2555 (1996).
- [19] K. Deligiannis et al., Phys. Rev. Lett. **79**, 2121 (1997).
- [20] R. Cubitt et al., Nature **365**, 407 (1993).
- [21] H. Safar et al., Phys. Rev. B **52**, 6211 (1995).
- [22] S. Ryu, A. Kapitulnik and S. Doniach, Phys. Rev. Lett. **77**, 2300 (1996).
- [23] H. Safar et al., Phys. Rev. Lett. **70**, 3800 (1993).
- [24] W. K. Kwok et al., Phys. Rev. Lett. **73**, 2614 (1994).
- [25] E. Jagla and C. Balseiro, Phys. Rev. Lett. **77**, 1588 (1996).
- [26] N. Wilkin and H. Jensen, Phys. Rev. Lett. **79**, 4254 (1997).
- [27] C. Wengel and A. Young, Phys. Rev. B **56**, 5918 (1997).
- [28] T. Giamarchi and P. Le Doussal, Phys. Rev. B **55**, 6577 (1997); A. Koshelev and V. Vinokur, cond-mat/9801144.
- [29] A. van Otterlo, R. T. Scalettar, and G. T. Zimányi, unpublished.
- [30] R. Koch et al., Phys. Rev. Lett. **63**, 1511 (1989).
- [31] D. Lopez et al., Phys. Rev. Lett. **80**, 1070 (1998).